

Optimization of Mobile Robotic Relay Operation for Minimal Average Wait Time

Winston Hurst, *Student Member, IEEE*, and Yasamin Mostofi, *Fellow, IEEE*

Abstract

This paper considers trajectory planning for a mobile robot which persistently relays data between pairs of far-away communication nodes. Data accumulates stochastically at each source, and the robot must move to appropriate positions to enable data offload to the corresponding destination. The robot needs to minimize the average time that data waits at a source before being serviced. We are interested in finding optimal robotic routing policies consisting of 1) locations where the robot stops to relay (relay positions) and 2) conditional transition probabilities that determine the sequence in which the pairs are serviced. We first pose this problem as a non-convex problem that optimizes over both relay positions and transition probabilities. To find approximate solutions, we propose a novel algorithm which alternately optimizes relay positions and transition probabilities. For the former, we find efficient convex partitions of the non-convex relay regions, then formulate a mixed-integer second-order cone problem. For the latter, we find optimal transition probabilities via sequential least squares programming. We extensively analyze the proposed approach and mathematically characterize important system properties related to the robot's long-term energy consumption and service rate. Finally, through extensive simulation with real channel parameters, we verify the efficacy of our approach.

Index Terms

Autonomous robots, Unmanned Aerial Vehicle (UAV), relay systems, communication-aware robotics, UAV-assisted communication, polling systems

I. INTRODUCTION

Significant advances in robotics over the past several years have created new possibilities in the design of communication systems. For example, unmanned vehicles (ground or unmanned aerial vehicles) may enable, extend, or improve networks via data muling [1–3], relaying [4–7], or beamforming [8, 9]. Design of these mobility-enabled communication systems must

Winston Hurst and Yasamin Mostofi are with the Department of Electrical and Computer Engineering, University of California, Santa Barbara, USA (email: {winstonhurst, ymostofi}@ece.ucsb.edu). This work was supported in part by NSF RI award 2008449.

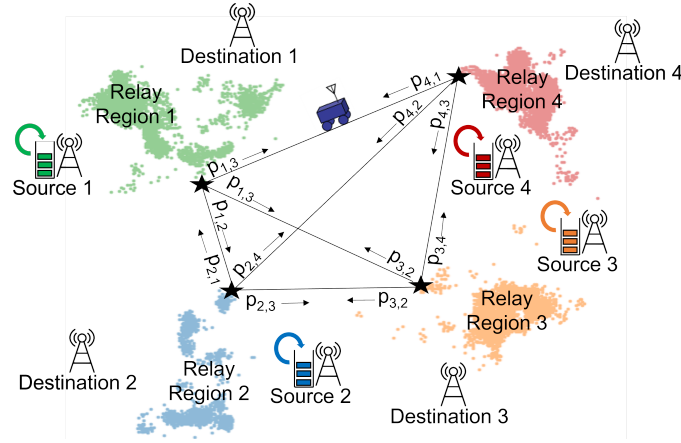


Fig. 1. At each source, data accumulates in a queue which must be offloaded to the corresponding destination while minimizing the average wait time. The relay operation is performed by a mobile robot, which needs to move to an optimum position within each feasible relay region to service the corresponding queue. After servicing queue i , the robot moves to service queue j with probability $p_{i,j}$, which is found based on optimizing a stochastic robotic routing policy. See the color pdf for better viewing.

account for both the motion and communication aspects of operation. This field is referred to as *communication-aware robotics* [10–13]. Muralidharan and Mostofi [13] provide a recent review of this area.

In this paper, we consider the operation of a mobile robot which is tasked with persistently servicing several disparate communication links each consisting of a source and destination pair, as shown in Fig. 1. Data arrives stochastically at each source and must be sent to its corresponding destination, which is too far away for direct communication. The mobile robot enables data transfer between each source-destination pair by creating a two-hop link between them. Examples of such systems include sensor networks [14] and ad hoc networks deployed for search and rescue or after a natural disaster.

To effectively operate, the robot must identify regions, labeled *Relay Regions* in Fig. 1, for each source-destination pair where the link qualities from (to) the source (destination) are good enough to permit the robot to relay data from the source to the destination. Then, the robot must plan a trajectory which repeatedly visits these regions, allowing for persistent data transfer.

Several factors make this problem interesting and complex. First, in general, full channel information is not known to the robot. Therefore, the robot must accurately predict the relay regions with limited information. Doing so requires realistic modeling of highly non-convex spatial variations of communication channels, based only on sparse prior samples, as simplified models, *e.g.*, disc models, may result in performance degradation. Second, as the real-world communication channels which determine the relay regions are irregular, the regions become

non-convex and disjoint, making path planning through them challenging. Third, the robot may need to service some pairs more frequently than others due to potential heterogeneous data accumulation rates and asymmetry in spatial locations. Fourth, the path planning needs to be co-optimized with transitional routing probabilities. Finally, persistent operation calls for infinite horizon planning, requiring careful trajectory parameterization and resource constraint definitions.

To account for these factors, we employ a realistic, probabilistic channel estimation framework and consider stochastic trajectories parameterized by a set of relay positions (one per relay region) and transition probabilities, as shown in Fig. 1. These *stochastic robotic path planning policies* allow for arbitrary, non-homogeneous service frequencies [15] and provide security benefits in adversarial settings [16]. Alternatively, they may be used as a basis for the construction of deterministic policies [17], which may be difficult to directly optimize.

Utilizing mobile robots to relay data has received considerable attention in recent years [1, 2, 18–23]. In these problems, trajectory optimization considers paths which either move the robot from node to node (data muling) [1, 2] or move the robot to locations where the wireless channel quality permits reliable communication [9, 20–23]. Closely related are persistent monitoring problems, in which a robot senses various locations in a workspace and transfers the sensed data to a remote station [24–28], and communication-aware variations of the vehicle routing problem (VRP) [29, 30].

However, servicing a number of source-destination pairs with heterogeneous traffic, and in real-world channel environments, through visit location optimization and persistent path planning differentiates this work from the literature. In much of existing work that addresses the robotic path planning component, either simplified channel models, *e.g.*, disc models, are used [6, 21, 24, 29], or the robot visits a number of sites directly, *i.e.*, without any communication component [1, 2].¹ This greatly simplifies optimization of visiting locations. Other work focuses on planning tours which visit each site exactly once [20, 26] rather than considering non-homogeneous visit frequencies. On the other hand, in most work that consider real communication issues, either path optimization from point A to point B is considered and/or only a single source-destination is assumed with a given starting point [31, 21–23, 9, 22]. Optimizing both the stop locations and the stochastic routing policy in realistic channel environments that result in highly non-convex

¹Note that the term "relaying" in these papers refers to data muling (physically picking data up from one location and dropping it off at another) and differs from what relaying means in this paper.

relay regions, and while addressing multiple heterogeneous, persistent sources introduces exciting new challenges, which motivates the proposed mathematical framework of this paper.

Our system of interest is also related to polling systems, in which a single server services multiple queues. In fact, we use seminal results which characterize average wait times for Markovian polling systems [32]. In fact, we show that polling system optimization becomes a special case of our problem of interest, and when appropriate, we draw analogies with polling system problems.

However, such work is not in the context of robotics, so issues related to location optimization and realistic communication environments are not relevant. Even without our robotic-related issues, a survey of polling systems literature shows that finding general optimal operating policies is an open problem [33–38]. The additional considerations of location optimization and realistic communication environments adds further complexity to our problem.

We next summarize our contributions.

- 1) For the highly non-convex and intractable persistent relaying problem described above, we introduce approximately-optimal robotic relay policies (AORP's) and bring a foundational understanding to this problem. Specifically, we propose a novel approach that iteratively minimizes the average wait time over both relay positions and the stochastic Markovian routing policy (i.e., robot transition probabilities from one service location to the next). These stochastic policies may be used as a basis for the construction of deterministic policies, as we shall also show.
- 2) When optimizing the service locations, we show how each relay region can be predicted and efficiently partitioned into a set of convex regions. We then show how the optimum robot service locations can be found via an efficient mixed-integer second-order cone program (MISOCP) that minimizes the average wait time. We further show how the optimum Markovian robotic routing policy can be found via sequential least squares programming (SLSQP).
- 3) Using a polling system model of the robot's operation, we mathematically characterize the robot's service time percentage, average power, and average service rate. As we shall see, our findings reveal interesting characteristics of the system in the long-term as well as the per stage context.
- 4) We extensively test the proposed approach in realistic channel environments (channel parameters from real data) and show the impact of several different parameters on the performance

of the system. We further compare with the state-of-the-art and also validate our theoretical results.

The rest of the paper proceeds as follows: Section II introduces models for communication, channel prediction, data accumulation and offloading, and robot motion, along with a Markov process model of the system. Section III formalizes the minimal average wait time problem, and in Section IV, we propose a novel algorithm to find approximately-optimal solutions. Section V provides analytical results on long-term energy consumption and service rate of the system. Section VI includes results from extensive simulated experiments which illustrate the efficacy of our approach, and we conclude in Section VII.

II. SYSTEM MODELING

Consider a single robot in an environment with n communication subsystems, each consisting of a pair of source-destination nodes, as shown in Fig. 1. Data arrives at each source node in a stochastic manner and needs to be communicated to its corresponding destination with a minimum delay. However, the source-destination pairs are located such that direct communication between them is not possible, possibly due to a large distance or blockage from objects in the environment. Thus, a mobile robot is tasked with acting as a relay, constantly planning its path in the area in order to transfer the information from each source to its corresponding destination while minimizing the overall delay. In this section, we present the models for communication, channel prediction, data transfer, and motion used in this paper, as well as a Markov chain model useful for analyzing long-term properties of the system.

A. Communication and Channel Prediction Model

Communication from a source to its destination involves data transfer across two channels: the link from the source to the robot and the link from the robot to destination. When the source (robot) transmits with power Γ_T , the received Signal-to-Noise Ratio (SNR) at the robot (destination) is given by $SNR_{\text{rec}} = \Gamma_T \times Y$, where Y is the Channel-to-Noise Ratio (CNR). The effects of path loss, shadowing, and multipath fading result in a spatially-varying CNR.

A minimum Bit Error Rate (BER) or other Quality of Service (QoS) requirement induces a minimum received SNR requirement for reliable communication, SNR_{th} . If $SNR \geq SNR_{\text{th}}$, the source (robot) can communicate with the robot (destination). Since the robot and the sources are assumed to have a fixed transmission power, the SNR threshold translates to a minimum required CNR threshold Y_{th} , and the spatially-varying channels dictate the connectivity regions.

In order for the robot to constantly plan its path and relay the information between the source-destination pairs, it needs to assess the connected region for each communication link, *i.e.*, the connected regions for communication from each source node to itself as well as the connected regions for transmission from itself to each destination. This, however, requires the robot to predict the channel quality at unvisited locations over the workspace. In this paper, we utilize our past work on stochastic channel prediction [39] to enable the robot to predict its connectivity regions. This approach uses a spatial stochastic process model that accounts for the effects of path loss, shadowing, and multipath fading. More specifically, the channel is characterized by path loss parameters θ , shadowing power α^2 , shadowing decorrelation distance β , and multipath fading power σ^2 . Given a very small number of prior channel measurements, the CNR (in dB) at an unvisited location x , $Y_{\text{dB}}(x)$, can then be best modeled by a Gaussian random variable with its mean and variance given as follows:

$$\mathbb{E}[Y_{\text{dB}}(x)] = H_x \hat{\theta} + \Psi^T(x) \Phi^{-1} (Y_m - H_m \hat{\theta}), \quad (1)$$

$$\Sigma(x) = \hat{\alpha}^2 + \hat{\sigma}^2 - \Psi^T(x) \Phi^{-1} \Psi(x),$$

where $Y_m = [y_1, \dots, y_m]^T$ are the m priorly-collected CNR measurements (in dB), $X_{\text{msr}} = [x_1^{\text{msr}}, \dots, x_m^{\text{msr}}]$ are the measurement locations, $\hat{\theta}$, $\hat{\alpha}$, $\hat{\beta}$, and $\hat{\sigma}$ are the estimated channel parameters (using Y_m), $H_x = [1 - 10\log_{10}(\|x - x_b\|)]$ with x_b denoting either the location of the source in the source-to-robot channel or destination in the robot-to-destination channel, $H_m = [H_{x_1^{\text{msr}}}^T, \dots, H_{x_m^{\text{msr}}}^T]^T$, $\Psi(x) = [\hat{\alpha}^2 \exp(-\|x - x_1^{\text{msr}}\|/\hat{\beta}), \dots, \hat{\alpha}^2 \exp(-\|x - x_m^{\text{msr}}\|/\hat{\beta})]^T$, and $\Phi = \Omega + \hat{\sigma}^2 I_m$ with $[\Omega]_{i,j} = \hat{\alpha}^2 \exp(-\|x_i^{\text{msr}} - x_j^{\text{msr}}\|/\hat{\beta})$, $\forall i, j \in \{1, \dots, m\}$ and I_m denoting the $m \times m$ identity matrix.

This Gaussian process model allows for the calculation of the probability that the CNR exceeds the minimum CNR imposed by the QoS requirement. Specifically, at point x : $\mathbb{P}(Y_{\text{dB}}(x) \geq Y_{\text{th, dB}}) = \mathbb{Q}((Y_{\text{th, dB}} - \mathbb{E}[Y_{\text{dB}}(x)])/\sqrt{\Sigma(x)})$, where $\mathbb{Q}(\cdot)$ represents the complementary cumulative distribution function of the standard normal distribution. The prior channel measurements required to make this prediction can be provided by static sensors in the field, gathered in previous operations or at the beginning of the operation, and/or obtained via crowdsourcing.²

The robot can only service the sources from locations where the CNR for both the source-to-robot and robot-to-destination channels exceed the threshold $Y_{\text{th, dB}}$. We call this the *true relay*

²The prior channel measurements that the robot can obtain are based on the downlink channel. When it needs to predict the uplink channel, the prior measurements can be collected by the remote sensor which can then send the needed parameters back to the robot for uplink channel prediction.

region: $R_i^{\text{true}} = \{x \in \mathbb{R}^2 | \Upsilon_{i,s,\text{dB}}^{\text{true}}(x) \geq \Upsilon_{\text{th,dB}}, \Upsilon_{i,d,\text{dB}}^{\text{true}}(x) \geq \Upsilon_{\text{th,dB}}\}$, where $\Upsilon_{i,s,\text{dB}}^{\text{true}}(x)$ and $\Upsilon_{i,d,\text{dB}}^{\text{true}}(x)$ are the true CNR in dB at location x of, respectively, the source-to-robot and robot-to-destination channels for the i^{th} source-destination pair.

The robot, however, will not know R_i^{true} and must predict the relay regions with the above channel prediction framework. Assuming independent channels, the probability of a successful communication between the i^{th} source-destination pair with the robot at position x is

$$p_{i,\text{sd}}(x) = \text{P}(\Upsilon_{i,s,\text{dB}}(x) \geq \Upsilon_{\text{th,dB}}) \times \text{P}(\Upsilon_{i,d,\text{dB}}(x) \geq \Upsilon_{\text{th,dB}}), \quad (2)$$

where $\Upsilon_{i,s,\text{dB}}(x)$ and $\Upsilon_{i,d,\text{dB}}(x)$ are the predicted CNR in dB at location x of, respectively, the source-to-robot and robot-to-destination channels for the i^{th} source-destination pair. By applying a threshold to the probability of successful end-to-end communication, p_{th} , we then have a *predicted relay region*: $R_i = \{x \in \mathbb{R}^2 | p_{i,\text{sd}}(x) \geq p_{\text{th}}\}$. Due to the irregular spatial variations of real-world communication channels, these regions will be highly non-convex.

All links are assumed to be of bandwidth B Hz, and both the source and robot transmit with a fixed spectral efficiency of ξ bps/Hz, *e.g.*, they transmit with a fixed M-QAM constellation. As a result, when servicing, the robot offloads data from the source at a rate of $\xi \times B$ bps.

B. Data Accumulation and Offloading

Let $\{q_1, \dots, q_n\}$ represent infinite-capacity queues at the sources. We assume that the data arrive at q_i according to a Poisson process with average rate λ_i bps. The *traffic* for a single queue is denoted by $\rho_i = \lambda_i \zeta$. For the entire system, we have $\lambda_s = \sum_{i=1}^n \lambda_i$ and $\rho_s = \sum_{i=1}^n \rho_i$.

The *average wait time*, \bar{W} , is the average duration of time between the moment a bit arrives in the queue and the moment it begins to be sent, and the *service time*, $\zeta = 1/(\xi B)$, is the time required to transfer a single bit from source to the robot, assuming a successful transmission, which will be part of the optimization framework. Thus, the average total time between the moment a bit enters a queue and the moment it arrives at the destination is $\bar{W} + 2\zeta$. The *service discipline* describes how many bits to service during a single visit to a source-destination pair. We consider the exhaustive service policy, in which the robot continues service until the queue is empty. For any robotic routing policy, this service discipline minimizes average wait time [35].

C. Motion Model

We assume that when in motion, the robot travels at a constant velocity, and we model the motion power as a linear function of speed. Specifically, we use a model derived from experimental studies which holds for a large class of robots (*e.g.*, Pioneer robots) [40]: $\Gamma_m(v) =$

$\kappa_1 v + \kappa_2$ for $v > 0$ and $\Gamma_m(v) = 0$ for $v = 0$, where v is the robot's speed, and κ_1 and κ_2 are positive constants determined by the robot's load and mechanical system. We consider trajectories where, for each pair, the robot chooses a single *relay position*, $r_i \in R_i$, at which the robot stops to relay, so that when traveling between two relay positions r_i and r_j , the motion energy consumed is given by $\mathcal{E}_m = (\kappa_1 + \kappa_2/v) \|r_i - r_j\|$.

The *robotic routing policy* determines the sequence in which the pairs are serviced. As discussed in Section I, we are interested in stochastic robotic routing policies characterized by an irreducible Markov chain, \mathcal{Q} , with a transition matrix P , where $p_{i,j}$ is the probability of servicing the j^{th} source-destination pair next, given the robot is currently servicing the i^{th} pair. We denote with $\pi = [\pi_1, \dots, \pi_n]$ the stationary distribution of \mathcal{Q} .

The *switching time* is the duration of time between the moment the robot completes service for one pair and begins service at the next. Let S denote the symmetric matrix of switching times, with $s_{i,j}$ denoting the switching time between q_i and q_j . The switching times are determined by the relay positions and the robot's speed: $s_{i,j} = \|r_i - r_j\|/v$. We write $S(X_r)$ to convey the dependency of S on $X_r := \{r_1, \dots, r_n\}$.

D. Markov Chain Model for Persistent Operation

The instant the robot begins to service a queue is referred to as a *polling instant*, and the duration of the robot's operation may be decomposed into a sequence of *stages*, with the k^{th} stage beginning and ending at the k^{th} and $(k + 1)^{\text{th}}$ polling instants, respectively. Let $L_k = [L_{1,k}, \dots, L_{n,k}]^T$ and $Q_k \in \{q_1, \dots, q_n\}$ denote the queue length at each source and the source being polled, respectively, at the k^{th} polling instant. The sequence of random variables $\mathcal{L} := \{(L_k, Q_k)\}_{k \geq 0}$ forms a Markov chain, and for the robotic routing policy and service discipline discussed above, the chain is stable, *i.e.*, positive recurrent, under the mild assumption that $\rho_s < 1$ and \mathcal{Q} is irreducible [41]. Thus, empirical time averages of system properties converge to the expected values indicated by the unique stationary distribution.

Analyzing the system via the properties of the Markov chain's stationary regime assumes that robotic operation is of sufficient duration for system metrics to approach the values predicted by an asymptotic analysis. In practice, this time is typically short.

The average wait time in the stationary regime is a function of the average arrival rates, service time, switching times, and transition probabilities. Specifically, we have the following lemma:

Lemma 1. *The average wait time \bar{W} in a polling system under the exhaustive service policy and a Markovian routing policy is given by:*

$$\bar{W}(\lambda, \zeta, S, P) = \underbrace{\frac{\rho_s \zeta}{2(1 - \rho_s)}}_{M/G/1 \text{ wait time}} + \underbrace{\frac{1}{2\bar{s}} \sum_{i=1}^n \pi_i \sum_{l=1}^n p_{ij} s_{i,j}^2 + \frac{1}{\bar{s}\rho_s} \sum_{i=1}^n \pi_i \sum_{j=1}^n p_{ij} s_{i,j} \sum_{k \neq i} \rho_k \bar{T}_{ki}}_{\text{additional wait time due to non-zero switching times}} \quad (3)$$

with $\bar{s} = \sum_{i=1}^N \pi_i \sum_{j=1}^N p_{ij} s_{i,j}$ denoting the average switching time and \bar{T}_{ki} denoting the expected time between any departure from q_i and the most recent previous departure from q_k . Note that \bar{T}_{ki} is a function of P and can be found by solving a system of n^2 equations.

Proof. The proof proceeds by first decomposing total wait time into the wait time of an equivalent $M/G/1$ queue and additional wait time incurred due to switching. This is then followed by a long derivation. See Boxma and Weststrate for details [37]. [32], \square

In the context of our relay system, ζ is fixed and given by the spectral efficiency and communication bandwidth. Switching times, $S(X_r)$, are determined by the robot's velocity, v , and the choice of relay positions, X_r . The relay positions are chosen from the relay regions, R_i , which are in turn determined by the spatially-varying channel qualities, the QoS requirements, and the transmission power Γ_t . The transition probabilities P are precisely the robotic routing policy, while the arrival rates λ_i are exogenous. Thus, given the spectral efficiency, ξ , channel bandwidth, B , the robot's velocity v , and the robotic relay policy (X_r, P) , we can calculate average wait time in the stationary regime as $\bar{W}(\lambda, 1/(\xi B), S(X_r), P)$ using Lemma 1.

III. PROBLEM FORMULATION

Consider our problem of a robot tasked with relaying data between n source-destination pairs. As mentioned earlier, an important performance metric of such a robotic relay system is the average wait time. Therefore, our objective is to minimize the system-wide average wait time³ as given in Eq. (3). Our problem is formally stated as:

$$\begin{aligned} \min_{X_r, P} \quad & \bar{W}(\lambda, \zeta, S(X_r), P) \\ \text{s.t.} \quad & P \in \mathcal{P}, \quad X_r \in \prod_{i=1}^n R_i \end{aligned} \quad (4)$$

where \mathcal{P} is the set of transition matrices describing irreducible Markov chains.

³We note that minimizing the maximum wait time can be another objective of interest, depending on the scenario [42, 43].

n	Number of source-destination subsystems	\bar{W}	Average wait time of the system
q_i	Queue at the source of the i^{th} subsystem	R_i	Predicted relay region of the i^{th} subsystem
r_i	Relay position of the i^{th} subsystem	\bar{s}	Average switching time
$S(X_r)$	Matrix of switching times between the relay positions	ζ	Service time, <i>i.e.</i> , time to transmit a single bit from source to destination
λ_i	Data arrival rate in bits per second for the i^{th} subsystem	λ_s	System-wide data arrival rate
ρ_i	Traffic of the i^{th} subsystem	ρ_s	System-wide traffic
P	Probability transition matrix for queue visits	π	Queue visit frequencies
$\Gamma_m(v)$	Motion power for velocity v	Γ_t	Transmit power
Q	Markov chain describing the sequence of queues serviced	\mathcal{L}	Markov chain with $\mathcal{L}_k = (L_k, Q_k)$ giving the queue lengths and queue serviced at the k^{th} polling instant, respectively.

TABLE I. List of Key Variables

Remark 1. *In Section V, we prove that long-term energy consumption (i.e., stationary values) does not depend on the robotic relay policy. On the other hand, as we shall see, per stage energy consumption is a function of the robotic relay policy. Sections IV-A and V-B show how our proposed approach implicitly minimizes average energy per stage.*

This problem, however, is challenging to analyze and solve due to the coupling of robotic path planning and data servicing. In fact, simpler versions of this problem, without the robotic component, are still difficult to analyze and have been the subject of extensive studies in both polling systems and queuing theory. We next present special cases of Problem (4) which motivate the rest of this paper and further put this optimization problem in the context of existing work.

A. Special Case: No Robotic Position Optimization

In this section, we briefly consider two special cases in which the robotic operation facet of our problem becomes irrelevant, so that (4) reduces to problems which have been studied extensively in queuing theory and polling systems. First, if the robot need not move at all, the solution to (4) may be found using results on M/G/1 queues, as stated in the following theorem:

Theorem 1 (M/G/1 equivalence for the case of no motion). *If $\mathcal{I} := \bigcap_{i=1}^n R_i \neq \emptyset$, then the $\{(X_r^*, P^*) | r_i^* = r_j^* \in \mathcal{I}, \forall i, j; P \in \mathcal{P}\}$ is the solution set of (4), and $\bar{W}^* = (\rho_s \zeta) / (2(1 - \rho_s))$ is the optimal value.*

Proof. If $\mathcal{I} := \bigcap_{i=1}^n R_i \neq \emptyset$, then all the predicted connected regions are overlapping. As such, the robot can stay in one location to service all source-destination pairs, *i.e.*, there is effectively no need for an unmanned vehicle. In this special case, all switching times become zero. As shown in [32], the polling system's wait time is minimized when all switching times are zero. We are thus left with an equivalent M/G/1 queuing system whose average wait time is given in the theorem, regardless of the transition probabilities. \square

Second, if each region R_i consists of only a single point, then optimization over relay positions becomes trivial. From the angle of minimizing average wait time, the relay system becomes mathematically equivalent to the polling system studied in [32]. No exact algorithm is known for this problem, and minimal wait times are found only through approximations [17, 44].

B. Coupled Path Planning and Communication Problem

While the results in Section III-A help root our work in existing literature, relay position optimization in those special cases is trivial. We now focus on the more realistic instances of Problem (4) in which relay positions must be optimized along with transition probabilities.

Among the many difficulties presented by this problem is the complex relationship between \bar{T}_{ki} and P . To better focus on the new dimension of path planning and avoid repeatedly solving the system of n^2 equations that relate \bar{T}_{ki} and P , we follow a common approach in polling systems literature [17] and restrict transition probabilities so that $p_{i,j} = p_{k,j} = \pi_j, \forall i, j, k \in \{1, \dots, n\}$, which we term a *stochastic* robotic routing policy. This permits a closed-form expression for \bar{T}_{ki} , as we characterize next:

Theorem 2. *For a polling system with stochastic routing, the expected time between any departure from q_i and the most recent previous departure from q_k is given by*

$$\bar{T}_{ki} = \frac{\rho_i \bar{t}}{\pi_i} + \bar{s}_i + \frac{(\rho_s - \rho_k) \bar{t}}{\pi_k} + \frac{1 - \pi_k}{\pi_k} \sum_{h=1}^n \pi_h \sum_{l \neq k} \pi_l s_{h,l}, \quad (5)$$

where \bar{t} is the average stage duration (mathematically characterized in Lemma 3 of Section V), and \bar{s}_i is the first moments of the switching time from any relay position to r_i .

Proof. See Appendix for the proof. \square

Stochastic robotic routing policies still allow for arbitrary visit frequency and security benefits while reducing the complexity of the design space. Robotic relay policies thus consist of the tuple (X_r, π) , and (4) can be restated as:

$$\begin{aligned}
& \min_{X_r, \pi} \bar{W}(\lambda, \zeta, S(X_r), P(\pi)) \\
& \text{s.t.} \quad \sum_{i=1}^n \pi_i = 1, \quad \pi_i > 0, \forall i, \quad X_r \in \prod_{i=1}^n R_i \quad .
\end{aligned} \tag{6}$$

where $P(\pi)$ indicates the dependence of P on π .

We refer to π_i as the *visit frequency* of q_i . We are then interested in finding the visit frequencies and relay positions that minimize average wait time, which is simpler than the original problem in (4). This problem, however, is still quite challenging and lacks structure that would make it easily solvable. In the next section, we then show how to find approximately-optimal solutions.

IV. APPROXIMATELY-OPTIMAL ROBOTIC RELAY POLICIES

The optimization problem in (6) is intractable due to the highly non-convex nature of the relay regions R_i and the strong coupling between X_r and π . Thus, it is necessary to find *approximately-optimal* robotic relay policies (AORP's). To reduce complexity, we propose an iterative approach which minimizes the average switching time over X_r with π fixed, then minimizes \bar{W} over π with X_r fixed. This may be repeated until convergence. Algorithm 1 outlines the approach. We denote the variables associated with the solution to Algorithm 1 with the AORP superscript, so the visit frequencies, robotic relay positions, and average wait time corresponding to the AORP are given by π^{AORP} , X_r^{AORP} , and \bar{W}^{AORP} , respectively. We next discuss the two stages of this approach in detail.

Algorithm 1: Approximately-Optimal Robotic Relay Policy (AORP)

Result: $\pi^{\text{AORP}}, X_r^{\text{AORP}}$

For each source-destination pair:

Step 1: Find the predicted relay regions (R_i), using the channel prediction model of

Section II-A.

Step 2: Find a_i , the α -shape of R_i .

Step 3: Simplify a_i using Ramer-Douglas-Peucker algorithm.

Step 4: Find convex partition of a_i using Hertel-Mehlhorn algorithm.

Initialize π^{AORP} with Eq. 12. Then iteratively optimize π^{AORP} and X_r^{AORP} :

Step 5: Solve Problem 10 to update X_r^{AORP} .

Step 6: Solve Problem 11 to update π^{AORP} .

Step 7: Repeat steps 5 and 6 until convergence.

A. Optimization of Robotic Path Planning

In the first part of our iterative approach, we fix π and find the optimal robotic relay positions X_r , simplifying (6) to:

$$\begin{aligned} \min_{X_r} \quad & \bar{W}(\lambda, \zeta, S(X_r), P(\pi)) \\ \text{s.t.} \quad & X_r \in \prod_{i=1}^n R_i \quad , \end{aligned} \quad (7)$$

In general, this problem is non-convex and intractable. In this section, we then show how we can tackle this problem. We first note that relay positions, X_r , affect the average wait time, \bar{W} , through the switching times, $s_{i,j}$. Specifically, compared to the wait time of the system with no switching times (*i.e.*, an M/G/1 queue), the average additional wait time due to switching times is positive everywhere except when the average switching time is zero ($\bar{s} = 0$), as discussed in the proof to Theorem 1. Therefore, an intuitive heuristic simplification for solving (7) is to minimize the average switching time instead. Furthermore, minimizing the average switching time amounts to minimizing the average distance traveled per stage of operation, which is a common objective in robotics. In fact, as we show in Section V-B, this is equivalent to minimizing average energy consumed per stage. Thus, rather than solving (7), we find X_r that minimizes the average switching time, as follows:

$$\min_{X_r, S} \quad \sum_{i=1}^n \pi_i \sum_{j=i}^n \pi_j s_{i,j} \quad (8a)$$

$$\text{s.t.} \quad \|r_i - r_j\|_2 = v s_{i,j}, \quad \forall i, j \quad (8b)$$

$$X_r \in \prod_{i=1}^n R_i \quad . \quad (8c)$$

The objective is linear, and if (8b) is relaxed, *i.e.*, $\|r_i - r_j\|_2 \leq v s_{i,j}$, it becomes a second-order cone constraint which will be active at the optimal solution. We next show how to partition the regions R_i so that (8c) can be stated as a combination of linear and integer constraints, making the problem a mixed-integer second-order cone program (MISOCP).

1) *Relay Region Partitioning:* In real channel environments, each relay region and predicted relay region can be irregular and non-convex in its shape. However, there are many clear advantages to optimizing over well defined regions in \mathbb{R}^2 . Thus, to solve (8) efficiently, we next propose a procedure, illustrated in Fig. 2, which converts each set R_i into a set of convex polygons $C_i = \{C_1^i, \dots, C_{m_i}^i\}$ whose union approximates the predicted relay region R_i .⁴

⁴As seen in Section VI, each R_i is not necessarily a joint set.

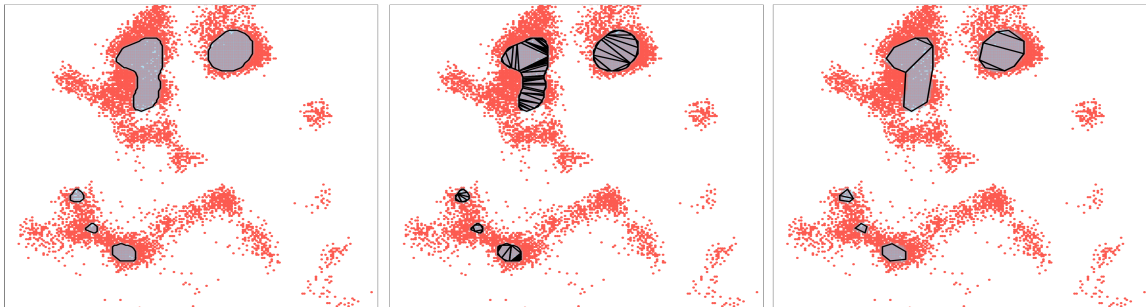


Fig. 2. Extraction of a convex partition of the predicted relay region. First, evaluating the probability of connectivity across a fine grid produces a set of points R_1 at which $p_{1,\text{sd}} > p_{\text{th}}$. Here $p_{\text{th}} = 0.7$, and R_1 is shown shaded in grey on top of the true relay region, shown in red. (Left) Extracting the α -shape of R_1 produces several non-convex polygons, 5 in this case. Then the resulting polygons are partitioned into convex regions using the Hertel-Mehlhorn algorithm. (Center) Without RDP smoothing, this produces 113 convex polygons. (Right) Using RDP to smooth before performing the partition reduces the number of polygons to 11. See the color pdf for better viewing.

- i Convert the points R_i to a set of (possibly non-convex and non-simple) polygons. This may be achieved by finding the α -shape of the points, as originally proposed in [45]. The α -shape of a set of points is a set of polygons that best fit the original set, where the value of α is chosen based on the granularity of the grid to make the resulting polygons as tight to the points as desired.
- ii Smooth the non-convex polygons using the Ramer-Douglas-Peucker (RDP) algorithm ([46, 47]). This will reduce the number of convex polygons required for partitioning. Tolerance on the amount of area lost or added by smoothing is set by the corresponding RDP parameters.
- iii Finally, perform convex partitioning on each of the smoothed polygons. A number of algorithms exist for such a partitioning. We elect to use the Hertel-Mehlhorn algorithm [48], which has a time complexity of $O(n)$ and is guaranteed to produce at most four times the minimal number of convex polygons required for the partition.

This approach produces a reasonable number of convex partitions that fit tightly to the predicted relay region, as illustrated in Fig. 2. The procedure is performed only once for each source-destination pair, and the same partitions are then used in each iteration of Algorithm 1.

2) *Mixed Integer Second-Order Cone Problem Formulation:* With the convex partitions, we can now reformulate (8) as a MISOCP. First, note that for each convex polygon C_k^i , there exists A_k^i, b_k^i , such that $A_k^i r_i - b_k^i \leq \mathbf{0}_n$ if and only if r_i is in C_k^i , where $\mathbf{0}_n$ indicates a vector of length n of all 0's, and with an abuse of notation, ' \leq ' is the entry-wise comparison. Furthermore, we introduce a set of indicator variables η_k^i , where $\eta_k^i = 1$ if $r_i \in C_k^i$ and $\eta_k^i = 0$ otherwise, and η

is the collection of all η_k^i . Then, we have the following mixed-integer program (MIP):

$$\min_{X_r, S, \eta} \sum_{i=1}^n \pi_i \sum_{j=i}^n \pi_j s_{i,j} \quad (9a)$$

$$\text{s.t.} \quad \|r_i - r_j\|_2 \leq v s_{i,j}, \quad \forall i, j \quad (9b)$$

$$\eta_k^i (A_k^i r_i - b_k^i) \leq \mathbf{0}_n, \quad \forall i, k \quad (9c)$$

$$\sum_{k=1}^{m_i} \eta_k^i = 1, \quad \forall i, \quad \eta_k^i \in \{0, 1\}, \quad \forall i, k \quad (9d)$$

where constraints (9c) and (9d) guarantee $r_i \in R_i$. However, the quadratic constraint (9c) contains both continuous and integer variables, making the problem intractable for many MIP solvers. We next show how to make (9c) linear.

Let $r_{i,1}$ and $r_{i,2}$ denote the first and second coordinates of r_i , respectively, and let $R_{i,k,\min} = \min\{r_{i,k} \mid r_i \in R_i\}$ and $R_{i,k,\max} = \max\{r_{i,k} \mid r_i \in R_i\}$. First, we constrain r_i to be within the bounding box $\mathbb{B}_i = [R_{i,1,\min}, R_{i,1,\max}] \times [R_{i,2,\min}, R_{i,2,\max}]$. Then for some large constant $c_k^i > \max_{r_i \in B_i} (\|A_k^i r_i\|_\infty)$, let $\tilde{b}_k^i = b_k^i + c_k^i \mathbf{1}_n$, $\tilde{A}_k^i = [A_k^i, c_k^i \mathbf{1}_n]$, and $\tilde{r}_k^i = [r_i, \eta_k^i]^T$, with $\mathbf{1}_n$ a vector of 1's with length n . Then $\tilde{A}_k^i \tilde{r}_k^i - \tilde{b}_k^i \leq \mathbf{0}_n$ if and only if $\eta_k^i (A_k^i r_i - b_k^i) \leq \mathbf{0}_n$, and the problem can be rewritten as a MISOCP:

$$\min_{X_r, S, \eta} \sum_{i=1}^n \pi_i \sum_{j=i}^n \pi_j s_{i,j} \quad (10a)$$

$$\text{s.t.} \quad \|r_i - r_j\|_2 \leq v s_{i,j}, \quad \forall i, j \quad (10b)$$

$$\tilde{A}_k^i \tilde{r}_k^i - \tilde{b}_k^i \leq \mathbf{0}_n, \quad \forall i, k, \quad r_i \in \mathbb{B}_i, \quad \forall i \quad (10c)$$

$$\sum_{k=1}^{m_i} \eta_k^i = 1, \quad \forall i, \quad \eta_k^i \in \{0, 1\}, \quad \forall i, k \quad (10d)$$

The constraints in (10c) are now linear, so this problem can be solved with mathematical solvers which provide guarantees of optimality and finite time convergence.

B. Optimizing the Stochastic Robotic Routing Policy

In the second part of our iterative procedure, we fix X_r to focus on finding the optimum stochastic robotic routing policy π . As a result, the optimization problem of (6) simplifies to:

$$\begin{aligned} \min_{\pi} \quad & \bar{W}(\lambda, \zeta, S(X_r), P(\pi)) \\ \text{s.t.} \quad & \sum_{i=1}^n \pi_i = 1, \quad \pi_i > 0, \quad \forall i \end{aligned} \quad (11)$$

This problem is mathematically similar to the stochastic polling system optimization problem, and as discussed in Section III-A, no exact algorithm is known for solving it in its general form. Thus, similar to [17], we use successive quadratic approximations to find approximate solutions. Specifically, we use sequential least squares programming (SLSQP), which finds a local minimum. We next briefly discuss a special case from polling systems literature for which a closed form solution to (11) does exist, and discuss its potential relevance to our robotic routing problem.

1) *Square Root Rule Approximation:* For a polling system with exhaustive service, Poisson arrivals, and a stochastic robotic routing policy, if all switching times are identical, then average wait time becomes convex in π , and a closed-form solution exists for the optimal visit frequencies, as stated in the following lemma:

Lemma 2. *Let π^* be the visit frequencies which minimize the average wait time in a polling system with exhaustive service, Poisson arrivals, and stochastic routing. If $s_{i,j} = s_{k,l}$, $\forall i, j, k, l \in \{1, \dots, n\}$, then*

$$\pi_i^* = \frac{\sqrt{\rho_i(1-\rho_i)}}{\sum_{j=1}^n \sqrt{\rho_j(1-\rho_j)}} . \quad (12)$$

Proof. See [17]. □

While Eq. (12) results in a closed-form solution, it requires identical switching times. In our robotic routing context, this will only hold if all switching times are zero since $s_{i,i} = 0$. This then results in the trivial case discussed in Theorem 1. As such, this special case does not directly apply to our scenario. However, we have observed from extensive simulations that Eq. (12) is a good approximation when all switching times except the self-loops, $s_{i,i}$, are similar, *i.e.*, when $s_{i,j} \approx s_{k,l}$, $\forall i, j, k, l \in \{1, \dots, n\}$, $i \neq j, k \neq l$. In other words, Eq. (12) may be a good approximation if the optimum robotic relay positions become approximately equal distanced. We leave rigorous investigation of this approximation to future work.⁵

2) *Observed Transition Probabilities:* The visit frequencies π found by solving (11) are with respect to the discrete time Markov chain produced by taking snapshots of the system at polling instances, *i.e.*, \mathcal{Q} . Consider the robot immediately after it completes servicing source q_i . With

⁵Note that even if we assume there is some form of delay that results in non-zero $s_{i,i}$'s, such values would be negligible as compared to the time it takes for the robot to travel from one relay region to the next, which is what differentiates this problem from polling systems.

probability π_i , the robot then transitions back to servicing q_i . However, under the exhaustive service policy adopted in this paper (see Section II-B), q_i will be empty at this point, resulting in the robot eventually finding another source to service instantly (i.e., no time expires). As such, it makes sense to exclude the self loops for simplicity, as summarized next:

Remark 2. *The observed stochastic robotic routing policy is Markovian with transition probabilities \tilde{P} given by*

$$\tilde{p}_{ij} = \begin{cases} \frac{\pi_j}{\sum_{k \neq i} \pi_k} & \text{if } j \neq i, \\ 0 & \text{otherwise.} \end{cases} \quad (13)$$

Consequently, the robot is always observed leaving a relay position immediately upon service completion, and the observed visit frequencies, $\tilde{\pi}$, may be found by finding the stationary distribution associated with \tilde{P} , i.e., $\tilde{\pi}^T \tilde{P} = \tilde{\pi}^T$. These observed transition probabilities give clearer descriptions of the robotic relay's behavior and are used in Section VI to analyze the results of the simulated experiments.

C. A Derived Deterministic Robotic Relay Policy

After convergence, an additional step may be taken to produce a routing table policy based on the AORP in which the relay positions and visit frequencies are the same but the robot visits the pairs according to a deterministic, periodic (not cyclic) sequence determined by π^{AORP} , using the Golden Ratio rule [49]. We refer to this policy as the AORP-Table (AORPT). The AORPT policy eliminates the need to select the next source to service on the fly while ensuring the same visit frequencies. As the traditional state-of-the-art in robotics route design is also deterministic, we use the AORPT for comparison in Section VI. We next give a brief example.

Consider the case with four source-destination pairs with $\pi = [1/2, 1/4, 1/8, 1/8]$. The Golden Ratio Rule produces the following visit sequence for the robot to follow repeatedly:

$$(q_1, q_2, q_1, q_3, q_1, q_2, q_1, q_4) \quad . \quad (14)$$

The resulting policy is periodic but not cyclic. Furthermore, it spaces visits evenly throughout the period. To illustrate, consider an alternative sequence which satisfies the visit frequencies π :

$$(q_1, q_2, q_1, q_2, q_1, q_3, q_1, q_4) \quad . \quad (15)$$

Here the two visits to q_2 both occur in the first half of the sequence whereas in (14), the visits are evenly distributed.

In summary, in this section, we showed how to find approximately-optimal solutions to the optimization problem in (6). Our proposed approach first finds an efficient convex partition for each predicted relay region. It then iteratively optimizes the robotic relay positions to minimize average switching time while fixing the robotic routing policy, followed by optimizing average wait time over the routing policy (*i.e.*, visit frequencies) while fixing the relay positions. After convergence, the visit frequencies can further be translated to a deterministic policy for efficient robotic operation in the field.

V. LONG-TERM AVERAGE POWER CONSUMPTION AND SERVICE RATE

In this section, we present important system properties regarding the long-term average power consumption and service rate. The results further motivate the choice used for the optimization problem formulation of the past sections. Our analysis focuses on average values when operating in the stationary regime. Thus, the results hold both in expectation across an ensemble of realizations over a finite number of stages, with initial conditions drawn according to the stationary distribution of the Markov chain \mathcal{L} , and in averaging asymptotically over time for any realization of the process, regardless of initial conditions. We first prove that the percentage of time spent servicing is independent of the robotic relay policy (X_r, P) . We then use this finding to derive key results regarding average power consumption and service rate.

A. Relating Percentage of Time Servicing to System Traffic

We first examine the significance of the system traffic, ρ_s , more closely and show that it gives the long-term percentage of time the robot spends servicing bits in a queue. Recall that, as presented in Section II-D, robotic operation may be decomposed into a series of stages demarcated by the polling instants, and that \mathcal{L} is a Markov chain with \mathcal{L}_k giving the state of the system, *i.e.*, the queue lengths and current queue under service, at the k^{th} polling instant. Recall further that the robotic relay system is stable in the sense that \mathcal{L} is positive recurrent if and only if $\rho_s < 1$ and \mathcal{Q} is irreducible. We are now ready to present the following lemma:

Lemma 3. *For any stable robotic relay policy, average stage duration in the stationary regime, \bar{t} , is given by $\bar{t} = \bar{s}/(1 - \rho_s)$, where \bar{s} is the average switching time.*

Proof. Under the assumption of stability, the average number of bits entering the system in a stage, $\bar{t}\lambda_s$, equals the average number leaving, $(\bar{t} - \bar{s})/\beta$. The result follows directly. \square

As \bar{s} is determined by our robotic relay policy, the average stage duration and the average time spent servicing during a single stage are likewise determined by the policy. However, Lemma 3

also indicates that the proportion \bar{s}/\bar{t} is fixed (equal to ρ_s) regardless of robotic relay policy, and similarly, the long-term percentage of time spent servicing is independent of the policy, as stated in the following theorem. Here and throughout the rest of the section, we use ‘ $\stackrel{\text{a.S.}}{=}$ ’ to indicate almost sure equality, and t_o is the time of operation.

Theorem 3. *Under any stable robotic routing policy, the system traffic ρ_s gives the long-term percentage of time spent servicing, i.e., $\lim_{t_o \rightarrow \infty} \phi(t_o)/t_o \stackrel{\text{a.S.}}{=} \rho_s$, where $\phi(t_o)$ is the total time spent servicing during operation.*

Proof. $\phi(t_o)$ may be decomposed into the sum of all service times completed during the full stages and an additional service time completed for the current, incomplete stage. t_o may be decomposed similarly so that

$$\lim_{t_o \rightarrow \infty} \frac{\phi(t_o)}{t_o} = \lim_{t_o \rightarrow \infty} \frac{\left(\sum_{k=1}^{K(t_o)} \phi_k + \phi_\epsilon \right) / K(t_o)}{\left(\sum_{k=1}^{K(t_o)} t_k + t_\epsilon \right) / K(t_o)} \stackrel{\text{a.S.}}{=} \lim_{K \rightarrow \infty} \frac{\left(\sum_{k=1}^K \phi_k \right) / K}{\left(\sum_{k=1}^K t_k \right) / K} \stackrel{\text{a.S.}}{=} \frac{(\bar{t} - \bar{s})}{\bar{t}} = \rho_s, \quad (16)$$

where $K(t_o)$ is the number of complete stages after operation of duration t_o , ϕ_k is the time spent servicing during the k^{th} stage, ϕ_ϵ is any additional service time, t_k is the duration of the k^{th} stage, and t_ϵ is any additional time. The second equality holds because t_ϵ and ϕ_ϵ are almost surely finite and the remaining equalities hold due to the positive recurrence of \mathcal{L} as guaranteed by the assumption of stability. \square

B. Energy Consumption and Average Power

Consider average energy consumption over a single stage of operation, including both communication and motion energy. We have the following theorem:

Theorem 4. *For any stable robotic relay policy, the average energy consumed over a single stage while operating in the stationary regime, \bar{E}_{st} , is given by $\bar{E}_{st} = \bar{t}(\Gamma_m(v)(1 - \rho_s) + \Gamma_t \rho_s)$*

Proof. Note that $\bar{E}_{st} = \bar{s}\Gamma_m(v) + (\bar{t} - \bar{s})\Gamma_t$. The result follows directly from Lemma 3. \square

Recalling from Lemma 3 that \bar{t} is a linear function of \bar{s} , we see the energy *per stage* is a linear function of average switching time \bar{s} , which is in turn determined by the robotic relay policy (see Section II-B). In other words, the optimization problem in (7) amounts to minimizing the average energy consumed per stage, which is an important metric in robotics literature. We next move from stage-level analysis to formally consider the long-term average power consumption of the robot.

Theorem 5. *Let $\mathcal{E}(t_o)$ be the energy consumed during operation of duration t_o . Then under any stable robotic relay policy $\lim_{t_o \rightarrow \infty} \mathcal{E}(t_o)/t_o \stackrel{\text{a.s.}}{=} \Gamma_m(v)(1 - \rho_s) + \Gamma_t \rho_s$.*

Proof. Note that $\mathcal{E}(t_o) = (t_o - \phi(t_o))\Gamma_m(v) + \phi(t_o)\Gamma_t$, where the first and second terms give the motion and communication energy, respectively. The result then follows from Theorem 3. \square

While Theorem 5 is an asymptotic result, in practice it holds for a long enough period of time (corroborated by simulation results of Section VI), as summarized next:

Remark 3. *For operation over a sufficiently large but finite duration t_o , $\mathcal{E}(t_o)$ is well approximated by $\mathcal{E}(t_o) \approx (\Gamma_m(v)(1 - \rho_s) + \Gamma_t \rho_s)t_o$.*

C. System Long-Term Average Service Rate

The average number of bits serviced during a stage must equal the average number of bits that enter the system for any stable policy (see Lemma 3), which leads to the following:

Theorem 6. *Under any stable robotic relay policy, $\lim_{t_o \rightarrow \infty} d(t_o)/t_o \stackrel{\text{a.s.}}{=} \lambda_s$, where $d(t_o)$ is the total number of bits serviced during operation.*

Proof. From the assumption of stability, data in and data out must be equal in the long-term. \square

While Theorem 6 is an asymptotic result, we find in practice that the empirical service rate converges quickly to λ_s , which leads to the following remark:

Remark 4. *The total bits serviced during operation over a sufficiently large but finite duration t_o is well approximated by $d_{out}(t_o) \approx \lambda_s t_o$.*

Importantly, systems with identical average long-term service rates may have vastly different average wait times. As a trivial example, consider two systems which each service a single bit during operation over a fixed amount of time. The first services the bit immediately and then idles the remainder of the time, while the second idles for a time and then services the bit at the very end of operation. While the average service rate of the two systems is identical, the first system results in less wait time. As such, the average wait time is the key metric to consider when optimizing robotic operation.

VI. SIMULATION RESULTS

In this section, we demonstrate the performance and efficacy of our approach with extensive simulations in realistic channel environments. First, we discuss channel prediction and the

extraction of convex partitions from the predicted relay regions. We then extensively study the performance of our approach by showing the effect of various system parameters on the AORP. We further show that our proposed approach can significantly reduce the average wait time compared to the state-of-the-art. Finally, we discuss the average service rate and energy consumption of the AORP to corroborate Theorems 6 and 5.

In our implementation of Algorithm 1, (6) is solved using the SLSQP solver of SciPy 1.7.1, and (10) is solved with IBM CPLEX 12.9. To initialize π , we use the approximation in (12), and in all simulations, we keep the following system parameters fixed: channel bandwidth $B = 2$ Mhz, spectral efficiency $\xi = 8$ bits/s/Hz, robot's constant velocity $v = 1$ m/s, and motion power parameters $\kappa_1 = 7.2$ N and $\kappa_2 = 0.29$ W.

A. Relay Region Prediction

We first generate the source-robot and robot-destination communication channels using realistic channel parameters derived from real-world measurements in downtown San Francisco. The following channel parameters, introduced in Section II-A, are extracted from the real channel measurements of [50]: $\alpha^2 = 16$, $\beta = 2.09$ m, $\theta = [5.2 \text{ dB}, -7.5]^T$ and $\sigma^2 = 1.96$. Then, different channel instances are generated based on these parameters using the probabilistic channel generator described in [51]. Briefly, [51] utilizes a given set of path loss, shadowing and multipath parameters to generate a 2D channel whose underlying parameters match the given set. The robot and sources transmit with a power of $\Gamma_t = 100$ mW, the receiver noise power is -85 dBm, and the acceptable SNR threshold for all the channels is set to 33 dB. Given the transmit power, the SNR threshold translates to a CNR threshold of $\Upsilon_{\text{th, dB}} = 13$ dBm. This then dictates the true relay regions, which the robot does not know but needs to predict.

The robot then uses 1% a priori channel samples for each channel to predict the channel over the rest of the workspace, which is unvisited. Using the approach outlined in Section II-A, the robot predicts the relay regions by calculating the probability of successful end-to-end communication, $p_{i,\text{sd}}$, based on the CNR threshold (see Eqs. (1) and (2)).

B. Relay Region Convex Partitioning

We next show the process of extracting the convex partitions as proposed in Section IV-A1, which plays a central role in the optimization of robotic relay positions. Fig. 3 (a,b) shows an example of source-to-robot and robot-to-destination channels, generated with the aforementioned real-world parameters. The robot then uses 1% a priori channel samples and predicts the channel

at the rest of the workspace in order to calculate $p_{i,sd}$ across a fine grid of points. We construct the relay region by selecting those points for which $p_{i,sd} \geq p_{th}$. Fig. 3 (c-e) shows a true connected region and two samples of the predicted regions for two values of p_{th} . As can be seen, for $p_{th} = 0.9$, the prediction framework is more conservative in declaring a location as connected, resulting in a smaller predicted relay region. As expected, fewer convex partitions are required for $p_{th} = 0.9$.

The table then compares the probability of true connectivity as well as the number of associated convex partitions for three values of p_{th} . As can be seen, the predicted relay regions provide good approximations of the regions where the robot may successfully communicate with both the source and destination, *i.e.*, R_i^{true} . In particular, we see that the probability that a point in R_i is in R_i^{true} becomes higher as the threshold increases, as expected. We furthermore observe that the probability of true connectivity is larger than the threshold probability, *i.e.*, for $p_c = P(x \in R_i^{true} | x \in R_i)$, we have $p_c > p_{th}$. Finally, the number of convex partitions reduces as p_{th} increases, as expected.

Overall, as p_{th} increases, the chance that locations in the predicted relay region are truly connected goes up, and the number of convex polygons required to partition the region decreases, simplifying optimization problem (10). However, increasing p_{th} makes the channel prediction more conservative and can lead to inefficient robotic operation as larger areas of the true relay region are excluded from the predicted region (see Fig. 3 (d,e)). As a result, the robot travels longer distances than needed between relay positions. In the rest of the paper, we use $p_{th} = 0.7$ for the prediction of all relay regions.

C. Impact of System Parameters

This section explores the impact of several system parameters on our proposed approach. We start with a system of three source-destination pairs in order to show the impact of several different system parameters on the performance. We then increase the complexity and show the performance for a system consisting of six source-destination pairs.

1) *Traffic*: To isolate the effect of traffic distribution, consider the three-queue system with symmetric placement of the subsystems shown in Fig. 4 (we note that the relay regions' irregularity always introduces some asymmetry). In all three cases, system traffic is held constant at $\rho_s = 0.5$ while ρ_1 is varied, where ρ_i is the traffic at the i^{th} source (see Section II-B). The remaining traffic is split evenly between ρ_2 and ρ_3 . The AORP transition probabilities are shown

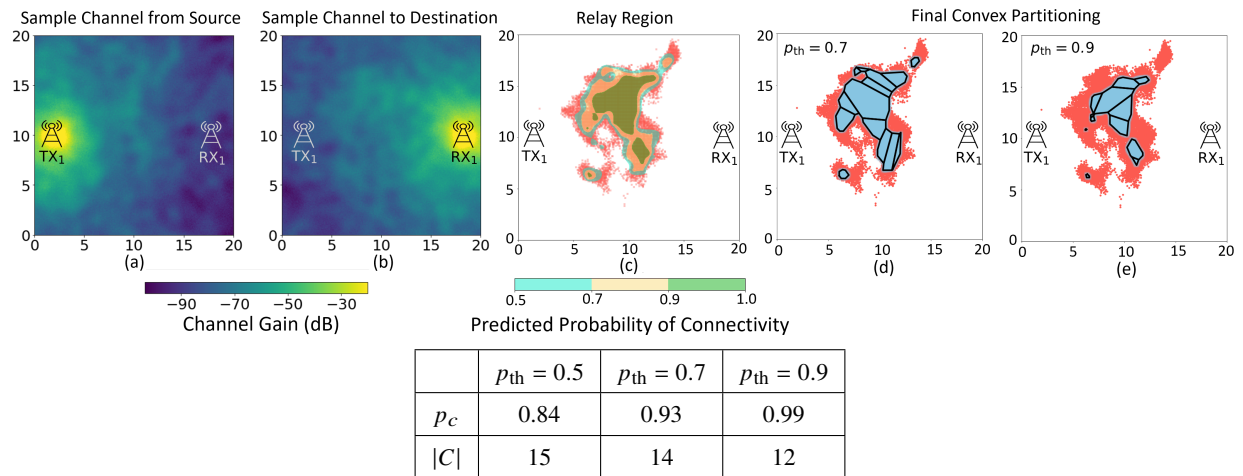


Fig. 3. Sample generated (a) source-to-robot and (b) robot-to-destination channels. The spatial variation of the channel is highly non-convex, as can be seen. (c) True relay region (red) and contours of predicted probability of successful end-to-end communication p_{sd} . (d,e) Final convex partitioning given two threshold probabilities p_{th} . The predicted relay regions (blue) are overlaid on the true relay region (red). (Bottom) The table shows p_c , the probability that a point in the predicted connected region is truly connected, and $|C|$, the number of convex partitions, for three values of p_{th} . See the color pdf for better viewing.

on the routes, observed visit frequencies and traffic are labeled on each subsystem, and the relay position within each predicted relay region is marked.

Intuitively, as the traffic ρ_i at q_i increases, $\tilde{\pi}_i^{\text{AORP}}$ should increase. As can be seen, with $\rho_1 = 0.1$, q_1 receives only half the traffic received by either q_2 or q_3 . Then, under the AORP, the robot mainly moves back and forth between q_2 and q_3 , visiting q_1 on average only once every four visits. When increasing ρ_1 so that the traffic of each queue is 0.17, $\tilde{\pi}_1^{\text{AORP}}$ increases so that the robot services each queue with approximately equal frequency. Finally, when $\rho_1 = 0.4$, q_1 receives four times the combined traffic of q_2 and q_3 . As can be seen, about half the visits are made to q_1 while the remaining are split between q_2 and q_3 . Furthermore, the relay positions r_2^{AORP} and r_3^{AORP} move farther away from each other to be closer to r_1^{AORP} since the robot will rarely switch between q_2 and q_3 . In summary, when a queue accounts for a greater proportion of the total system traffic, the visit frequency to that queue increases, and the relay positions may shift to account for certain switches occurring more frequently.

2) *Subsystem Placement*: The relative placement of each source-destination subsystem also greatly impacts the AORP, as shown in Fig. 5. To isolate the effect of subsystem placement, we keep the traffic at all subsystems equal. The subsystems are first placed so that midpoints between each source-destination pair form the vertices of an equilateral triangle. The first subsystem is then increasingly offset in the direction of the positive y-axis, as shown.

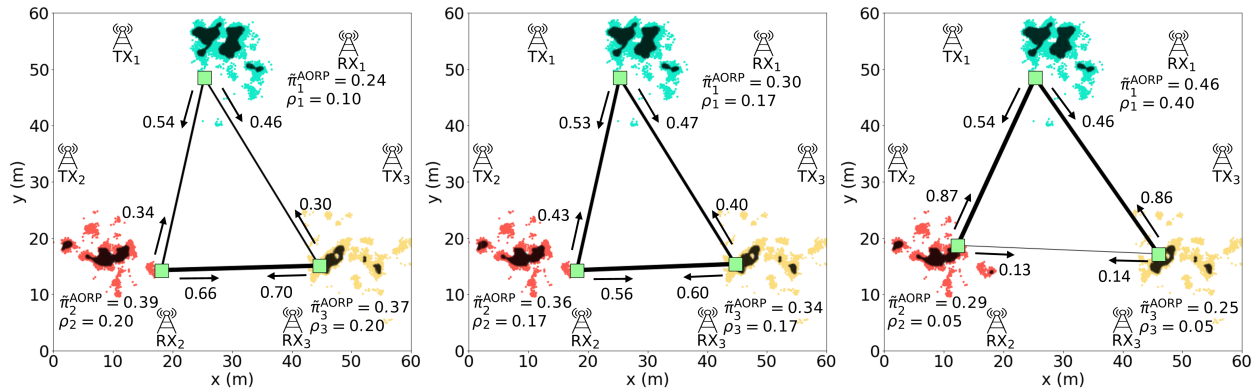


Fig. 4. Effect of traffic distribution on the AORP probability transitions and relay positions. The green squares indicate the relay positions, and the observed transition probabilities, $\tilde{p}_{i,j}^{\text{AORP}}$, are labeled on the arrows along each edge while the thickness of each edge corresponds to $\tilde{p}_{i,j}^{\text{AORP}}$ as well. Each subsystem is labeled with both the corresponding incoming traffic, ρ_i , and the resulting visit frequency, $\tilde{\pi}_i^{\text{AORP}}$. For each subsystem, the predicted relay region (in black) is overlaid on the true connected region. Moving from left to right, the increase in ρ_1 is reflected in the AORP transition probabilities and visit frequencies, as can be seen. See the color pdf for optimum viewing of this figure.

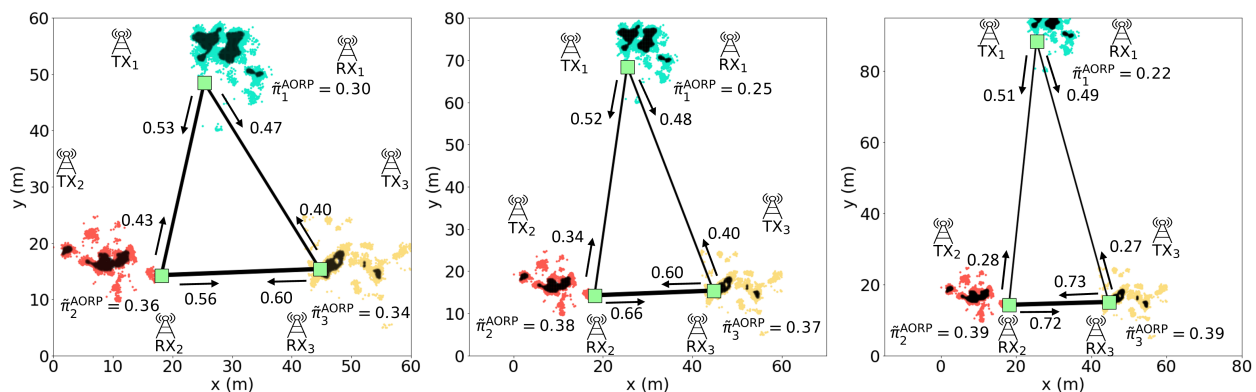


Fig. 5. Effect of subsystem placement on the AORP probability transitions and relay positions. The green squares indicate the relay positions, and the observed transition probabilities, $\tilde{p}_{i,j}^{\text{AORP}}$, are labeled on the arrows along each edge while the thickness of each edge corresponds to $\tilde{p}_{i,j}^{\text{AORP}}$ as well. In all cases, the traffic at each queue is $\rho_i = 0.17$. For each subsystem, the predicted relay region (in black) is overlaid on the true connected region. Moving from left to right, subsystem one is moved farther away from the rest of the subsystems, and the impact of its increased isolation is then reflected in the AORP transition probabilities and visit frequencies, as can be seen. See the color pdf for optimum viewing of this figure.

When the placement is symmetric (Fig. 5 (left)), each queue is serviced with approximately the same frequency. The slight difference in visit frequencies can be explained by the particular shape of the predicted relay regions, which are naturally different from each other. In other words, although the source-destination pairs are positioned symmetrically, different shapes and locations of the predicted relay regions result in r_2^{AORP} and r_3^{AORP} being placed closer to one another than either can be to r_1^{AORP} , thus making the switching time to q_1 relatively longer. As a result, q_1 is visited less frequently.

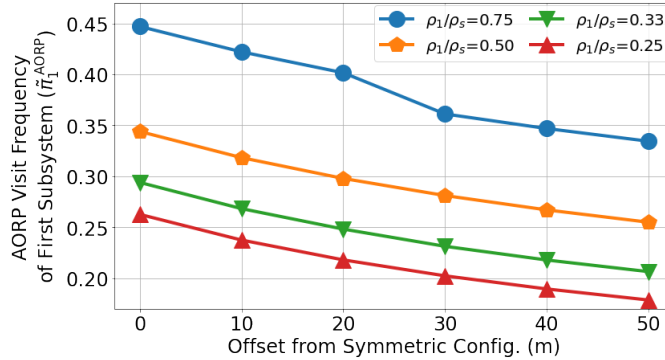


Fig. 6. Impact of subsystem placement on the observed visit frequency of the first subsystem under the AORP ($\tilde{\pi}_1^{\text{AORP}}$) for different traffic values, *i.e.*, for various values of the ratio ρ_1/ρ_s in the three-queue system. See the color pdf for optimum viewing of this figure.

As the first subsystem is offset by first 20 m and then 40 m in the subsequent figures, $\tilde{\pi}_1^{\text{AORP}}$ drops to 0.25, then 0.22, respectively. Intuitively, the optimum switching times $s_{2,1}$, $s_{1,2}$, $s_{3,1}$ and $s_{1,3}$ increase as q_1 moves farther away, so visits to q_1 lead to greater wait times in q_2 and q_3 . Thus, q_1 is visited less often as it becomes more isolated.

3) *Impact of Both Traffic and Subsystem Placement:* Fig. 6 shows the impact of both subsystem placement and varying traffic. An offset of 0 indicates the system is configured symmetrically, as in Fig. 5 (left), and increasing the offset moves the q_1 subsystem away from the original configuration, as shown in Fig. 5 (center, right). The overall system traffic ρ_s is constant across all experiments, and ρ_1/ρ_s gives the percentage of incoming traffic through q_1 , which is varying. The remaining traffic is split evenly between q_2 and q_3 so that traffic is symmetric when $\rho_1/\rho_s = 0.33$. The figure then shows the AORP observed visit frequency of the first subsystem ($\tilde{\pi}_1^{\text{AORP}}$). As can be seen, regardless of the distribution of traffic, moving subsystem one farther away, decreases $\tilde{\pi}_1^{\text{AORP}}$. Likewise, when less traffic arrives at q_1 , $\tilde{\pi}_1^{\text{AORP}}$ decreases regardless of offset.

4) *Velocity:* We next discuss the impact of the robot's speed on the performance of the AORP. Switching times scale linearly with the inverse of robot's velocity, *i.e.*, $1/v$, and as such, v significantly impacts the average wait time of the AORP. Specifically, Eqs. (3) and (5) indicate that wait time \bar{W} is an affine function of $1/v$ for any stochastic policy. This is seen in Fig. 7 (right), which shows the average wait time of the AORP as a function of the robot's speed in the three-queue system shown in Fig. 4 (right). Interestingly, as $v \rightarrow \infty$, $s_{i,j} \rightarrow 0$, $\forall i, j \in \{1, \dots, n\}$, and consequently \bar{W} converges to the wait time of an M/G/1 queue (see Theorem 1).

Fig. 7 further shows the queue lengths over the last four minutes of a two-hour operation

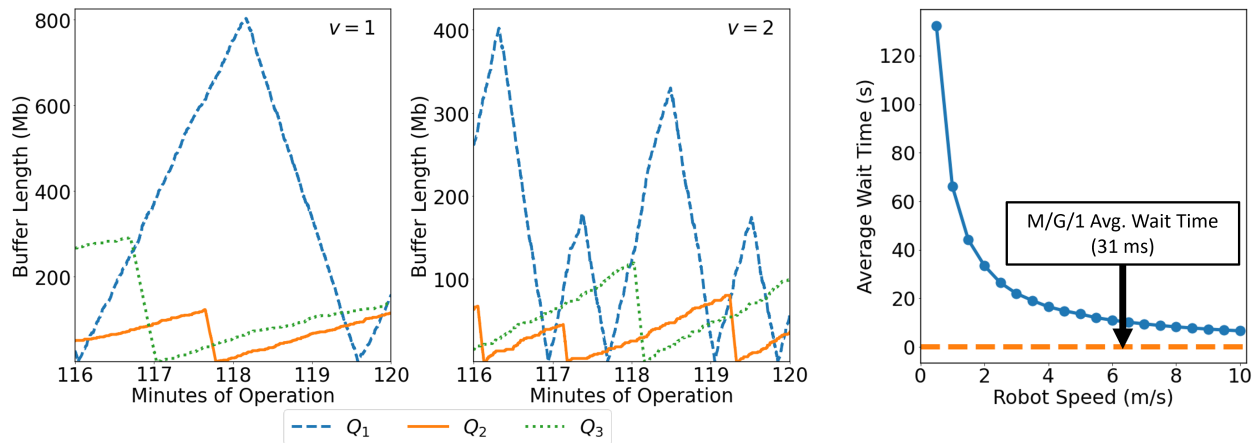


Fig. 7. Impact of robot velocity on wait times and queue lengths in a three-queue system. (Left, center) Sample realization of queue lengths during the last four minutes of a two-hour operation period for two sample velocities. The peaks (troughs) indicate polling (switching) instants. Larger v results in shorter stages and queue lengths. (Right) Increasing v also reduces overall average waiting time at a rate of $1/v$. See the color pdf for optimum viewing of this figure.

for $v = 1$ m/s (left) and $v = 2$ m/s (right). Doubling the velocity reduces all switching times by half, and as this shortens average queue lengths, the time spent servicing during a single stage decreases, too, as mathematically characterized in Section V. This results in the completion of approximately twice as many stages (*i.e.*, polling instances), as can be seen.

5) *A More Complex System:* To illustrate how the proposed AORP works in more complex scenarios, we next consider the system of six source-destination pairs shown in Fig. 8. The system consists of three high traffic queues (q_1 , q_2 , and q_3) and three low traffic queues (q_4 , q_5 , and q_6). Furthermore, the second and fifth subsystems are placed towards the center.

The table shows that while the relative traffic at each queue is somewhat reflected in the AORP visit frequencies, they are not exactly proportional due to different locations of the subsystems as well as the underlying space-varying channel quality. The three high traffic queues are visited most, and the edges traversed most frequently form a triangle with vertices given by the relay positions r_1^{AORP} , r_2^{AORP} , and r_3^{AORP} . Among the high (low) traffic queues, q_2 (q_5) is visited most often as it is located more centrally compared to q_1 and q_3 (q_4 and q_6). Consequently, when the robot moves from q_1 to q_3 , it will frequently stop at q_2 along the way. Furthermore, the particular channel realizations in the first, second, and third subsystems results in the second relay position, r_2^{AORP} , being placed closer to r_1^{AORP} than r_3^{AORP} . As a result, q_1 is visited more frequently than q_3 despite their symmetry in traffic and subsystem placement. Thus, we again see that the AORP accounts for the differing arrival rates, the relative positioning of the subsystems,

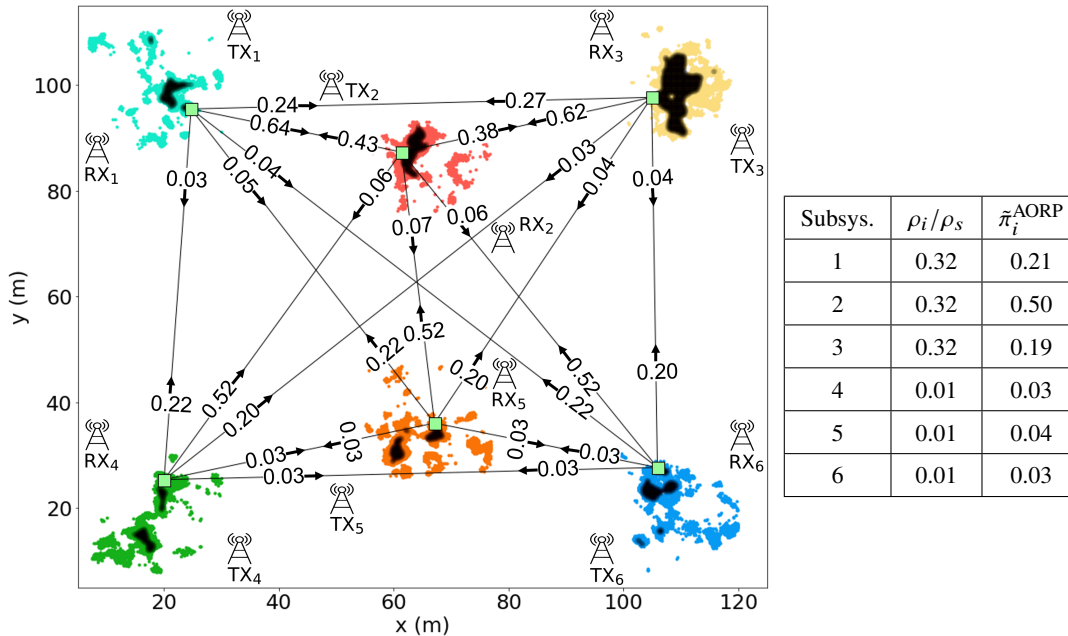


Fig. 8. (Left) The AORP for a six-queue system. For each subsystem, the predicted relay region (in black) is overlaid on the true connected region. The transmitter and receiver locations for each source-destination pair are marked, and green squares indicate the relay positions. The observed transition probabilities $\tilde{p}_{i,j}^{\text{AORP}}$ are labeled along each route. (Right) The table gives the percentage of traffic, ρ_i/ρ_s , and observed visit frequency, $\tilde{\pi}_i^{\text{AORP}}$, for each queue. See the color pdf for optimum viewing.

and the specific shape of the communication channels, even in more complex systems.

D. Comparison to the State-of-the-Art

We next compare our proposed robotic routing policy with a baseline approach that would be consistent with the state-of-the-art. To the best of our knowledge, the problem of interest to this paper is solved neither in the robotics nor in the communication literature, so we will use the solution proposed for a similar problem in the literature as a baseline. Specifically, visiting different relay regions in an efficient manner resembles a category of robotic path planning problems known as traveling salesperson problems with neighborhoods, which continues to be the basis of proposed solutions to several data gathering problems in robotics literature [1, 3, 26, 29, 52–54]. We then compare our approach with this baseline.

Consider the three-queue system shown in Fig. 9, with $\rho_1 = 0.32$, $\rho_2 = 0.04$, and $\rho_3 = 0.04$. Since the baseline is a deterministic policy, we compare it with AORP-Table as discussed in Section IV-C. For each policy, we simulate twenty two-hour operation periods with the queues initially empty. As shown in Fig. 9, the wait time under the baseline policy is 92.89 s, while under the AORP, it is 66.05 s. Thus the average wait time under the baseline policy is 26.84 s

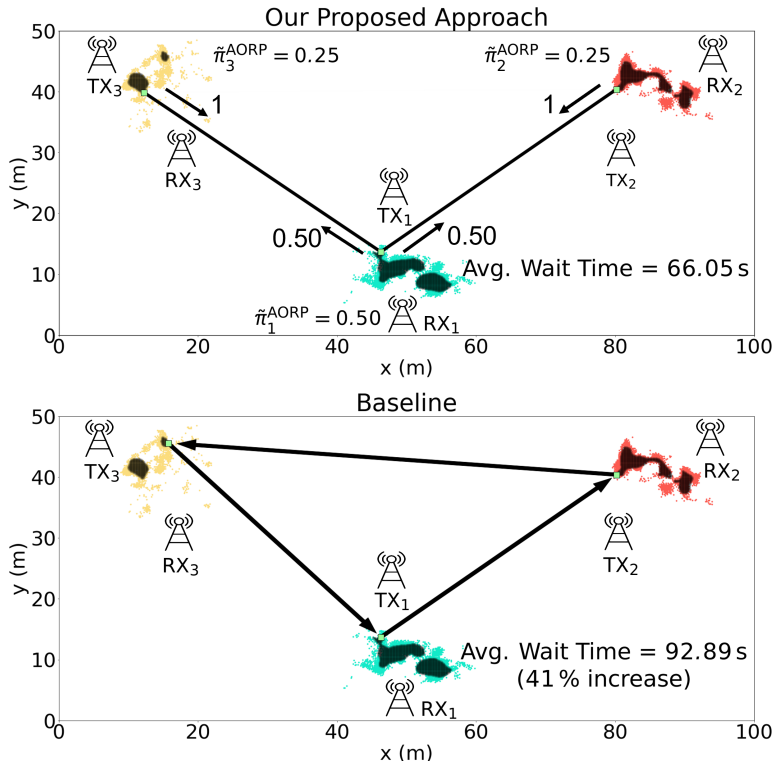


Fig. 9. Comparison of our proposed approach (top) and the baseline (bottom) for a three-pair system with $\rho = 0.32$ and $\rho_2 = \rho_3 = 0.04$. The observed probability transitions under the AORP, $\tilde{p}_{i,j}$, are labeled along each edge of the AORP, and the thickness of the line between relay positions indicates the relative frequency with which the edge is traversed. Under the AORP, $\tilde{p}_{2,3} \approx \tilde{p}_{3,2} \ll 0.01$, so for ease of presentation, we treat those probabilities as 0. See the color pdf for optimum viewing.

(41 %) longer than the average wait time under the AORP. This is achieved through a proper design that jointly considers the path planning and communication aspects of the problem, as we have proposed in this paper. We note that given the conservative bias of our prediction framework as discussed earlier, the probability of the relay positions being truly connected is very high. As such, the relay positions are assumed connected for both our approach and the baseline in the analysis of Fig. 9.

E. Confirmation of the Theories of Section V

Theorems 5 and 6 characterized the robot's average service rate and average operation power under a stable policy. We next confirm these theorems with our simulated data. Consider the three-queue system of Fig. 9. Again, we run twenty two-hour simulations, and for each simulation, record the average power and service throughput. The average power across all simulations is 4.58 W, consistent with the 4.53 W predicted by Theorem 5. Similarly, the average service rate from simulated data is 6.34 Mb/s, while Theorem 6 predicts it to be 6.40 mb/s.

As discussed in Section V, the overall average power and average service rate are independent of the robotic routing policy (assuming the policy is stable) when averaged over several stages of operation. To this end, we further note that the average power and service rate under the baseline policy were 4.61 W and 6.29 Mb/s, respectively, which is consistent with the theorems and remarks of Section V. As such, the average wait time is the right metric to consider when designing robotic relay policies, as we have done in this paper.

VII. CONCLUSIONS

This paper considered a mobile robot (ground or UAV) which relays data between pairs of otherwise far-away source and destination communication nodes. We posed the problem of finding the optimal stochastic robotic relay policy, consisting of visiting frequencies and relay positions. To find approximate solutions to this problem, we proposed a novel algorithm (AORP) which alternately optimizes average wait time over the visiting frequencies and average switching time over relay positions. To minimize the average switching time, we showed how to decompose the highly non-convex relay regions into efficient convex partitions, allowing us to formulate the problem as a MISOCP. Additionally, we mathematically characterized a number of important properties of the system related to the robot's long-term energy consumption and service rate. Through extensive simulations with real channel parameters, we showed how various system parameters affect the AORP and further compared with the state-of-the-art.

APPENDIX - PROOF OF THEOREM 2

Proof. We consider each term in the expression

$$\frac{\rho_i \bar{t}}{\pi_i} + \bar{s}_i + \frac{(\rho_s - \rho_k) \bar{t}}{\pi_k} + \frac{1 - \pi_k}{\pi_k} \sum_{h=1}^n \pi_h \sum_{l \neq k} \pi_l S_{h,l} .$$

Looking back in time, the process first serviced the data in q_i . From [55], the expected time to do so is $\rho_i \bar{t} / \pi_i$ (first term). Immediately preceding this, the robot switched to q_i (second term). With probability π_k , the queue serviced immediately prior to q_i was q_k . With probability $1 - \pi_k$, the queue just prior to q_i was not q_k , and we expect $1/\pi_k$ additional backward steps before reaching q_k . These steps consist of servicing and switching intervals. None of the servicing intervals occur at q_k , so the expected number of times q_j , $j \neq k$, is serviced is $[\pi_j / (1 - \pi_k)] / \pi_k$. Summing over all $j \neq k$, the contribution to \bar{T}_{ki} from these intervals is the third term. Similarly, we expect to have switched away from q_j a total of π_j / π_k times, but none of those switches will be to q_k . Thus the contribution to \bar{T}_{ki} from all these switching times is the fourth term. \square

REFERENCES

- [1] J. Zhou, J. Li, R. Q. Hu, and Y. Qian, "Study of visiting frequency in a delay tolerant network," in *2012 IEEE Int. Conf. on Commun.*, 2012, pp. 58–62.
- [2] K. H. Kabir, M. Sasabe, and T. Takine, "Optimal visiting order of isolated clusters in dtms to minimize the total mean delivery delay of bundles," *Numerical Algebra, Control and Optimization*, vol. 1, pp. 563–576, 2011.
- [3] O. Tsilomitrou, N. Evangeliou, and A. Tzes, "Mobile robot tour scheduling acting as data mule in a wireless sensor network," *2018 5th International Conference on Control, Decision and Information Technologies (CoDIT)*, pp. 327–332, 2018.
- [4] E. Carrillo, S. Yeotikar, S. Nayak, M. K. M. Jaffar, S. Azarm, J. W. Herrmann, M. Otte, and H. Xu, "Communication-aware multi-agent metareasoning for decentralized task allocation," *IEEE Access*, vol. 9, pp. 98 712–98 730, 2021.
- [5] Z. Zhang, B. Zhang, and Y. Wu, "Joint communication-motion planning in networked robotic systems," *Applied Sciences*, vol. 12, no. 12, 2022. [Online]. Available: <https://www.mdpi.com/2076-3417/12/12/6261>
- [6] J. Park, H.-H. Choi, and J.-R. Lee, "Flocking-inspired transmission power control for fair resource allocation in vehicle-mounted mobile relay networks," *IEEE Transactions on Vehicular Technology*, vol. 68, pp. 754–764, 2019.
- [7] S. Reveliotis and Y.-I. Kim, "Min-time coverage in constricted environments: Problem formulations and complexity analysis," *IEEE Transactions on Control of Network Systems*, vol. 9, no. 1, pp. 172–183, 2022.
- [8] A. Muralidharan and Y. Mostofi, "Energy Optimal Distributed Beamforming using Unmanned Vehicles," *IEEE Transactions on Control of Network Systems*, 2017.
- [9] S. Evmorfos, K. I. Diamantaras, and A. P. Petropulu, "Reinforcement learning for motion policies in mobile relaying networks," *IEEE Transactions on Signal Processing*, vol. 70, pp. 850–861, 2022.
- [10] A. Ghaffarkhah and Y. Mostofi, "Channel learning and communication-aware motion planning in mobile networks," in *Proc. American Control Conf.*, 2010.
- [11] A. Muralidharan and Y. Mostofi, "Path Planning for Minimizing the Expected Cost Until Success," *IEEE Trans. on Robot.*, vol. 35, no. 2, pp. 466–481, 2019.
- [12] —, "Statistics of the Distance Traveled until Connectivity for Unmanned Vehicles," *Autonomous Robots*, vol. 44, no. 1, pp. 25–42, 2020.
- [13] —, "Communication-aware robotics: Exploiting motion for communication," *Annu. Rev. of Control, Robot., and Auton. Syst.*, 2020.
- [14] D. Henkel and T. X. Brown, "Delay-tolerant communication using mobile robotic helper nodes," in *2008 6th International Symposium on Modeling and Optimization in Mobile, Ad Hoc, and Wireless Networks and Workshops*, 2008, pp. 657–666.
- [15] K. Srivastava, D. M. Stipanović, and M. W. Spong, "On a stochastic robotic surveillance problem," in *48th IEEE Conf. on Decision and Control held jointly with 2009 28th Chinese Control Conf.*, 2009, pp. 8567–8574.
- [16] J. Grace and J. Baillieul, "Stochastic strategies for autonomous robotic surveillance," in *44th IEEE Conf. on Decision and Control*, 2005, pp. 2200–2205.
- [17] O. Boxma, H. Levy, and J. Weststrate, "Efficient visit orders for polling systems," *Perform. Evaluation*, vol. 18, pp. 103–123, 1993.
- [18] S. Evmorfos, D. Kalogieras, and A. Petropulu, "Adaptive discrete motion control for mobile relay networks," *Frontiers in Signal Processing*, vol. 2, 2022. [Online]. Available: <https://www.frontiersin.org/articles/10.3389/frsip.2022.867388>
- [19] Y. Mostofi and R. Murray, "Effect of Time-Varying Fading Channels on the Control Performance of a Mobile Sensor Node," in *Proceedings of IEEE 1st International Conference on Sensor and Ad Hoc Communications and Networks (Secon)*, Santa Clara, CA, October 2004, pp. 317–324.

- [20] A. Ghaffarkhah and Y. Mostofi, "Dynamic Networked Coverage of Time-Varying Environments in the Presence of Fading Communication Channels," *ACM Trans. on Sensor Netw.*, vol. 10, no. 3, April 2014.
- [21] Z. Shen and H. Jiang, "Mobile relay scheduling in partitioned wireless sensor networks," *IEEE Transactions on Vehicular Technology*, vol. 65, pp. 5563–5578, 2016.
- [22] A. Pogue, S. Hanna, A. Nichols, X. Chen, D. Cabric, and A. Mehta, "Path planning under mimo network constraints for throughput enhancement in multi-robot data aggregation tasks," in *2020 IEEE/RSJ International Conference on Intelligent Robots and Systems (IROS)*, 2020, pp. 11 824–11 830.
- [23] J. George, C. T. Yilmaz, A. Parayil, and A. Chakraborty, "A model-free approach to distributed transmit beamforming," in *ICASSP 2020 - 2020 IEEE International Conference on Acoustics, Speech and Signal Processing (ICASSP)*, 2020, pp. 5170–5174.
- [24] J. L. Ny, M. Dahleh, E. Feron, and E. Frazzoli, "Continuous path planning for a data harvesting mobile server," in *47th IEEE Conf. on Decision and Control*, 2008, pp. 1489–1494.
- [25] Y. Khazaeni and C. G. Cassandras, "An optimal control approach for the data harvesting problem," in *54th IEEE Conf. on Decision and Control*, 2015, pp. 5136–5141.
- [26] J. R. Peters, A. Surana, G. S. Taylor, T. S. Turpin, and F. Bullo, "Uav surveillance under visibility and dwell-time constraints: A sampling-based approach," *ArXiv*, vol. abs/1908.05347, 2019.
- [27] S. Zhang, H. Zhang, L. Song, Z. Han, and H. V. Poor, "Sensing and communication tradeoff design for aoi minimization in a cellular internet of uavs," in *IEEE Int. Conf. on Commun.*, 2020, pp. 1–6.
- [28] S. C. Pinto, S. B. Andersson, J. M. Hendrickx, and C. G. Cassandras, "Multi-agent persistent monitoring of targets with uncertain states," *IEEE Transactions on Automatic Control*, 2022.
- [29] G. D. Çelik and E. Modiano, "Dynamic vehicle routing for data gathering in wireless networks," in *49th IEEE Conf. on Decision and Control*, 2010, pp. 2372–2377.
- [30] L. E. F. Luyo, A. Agra, R. Figueiredo, and E. O. Anaya, "Mixed integer formulations for a routing problem with information collection in wireless networks," *Eur. J. Oper. Res.*, vol. 280, pp. 621–638, 2020.
- [31] M. A. Abd-Elmagid and H. S. Dhillon, "Average peak age-of-information minimization in uav-assisted iot networks," *IEEE Transactions on Vehicular Technology*, vol. 68, pp. 2003–2008, 2019.
- [32] O. Boxma and J. Weststrate, "Waiting times in polling systems with markovian server routing," in *Messung, Modellierung und Bewertung von Rechensystemen und Netzen. Informatik-Fachberichte*, 1989.
- [33] E. Perel, N. Perel, and U. Yechiali, "A polling system with 'join the shortest - serve the longest' policy," *Comput. Oper. Res.*, vol. 114, 2020.
- [34] V. M. Vishnevsky, O. V. Semenova, and D. T. Bui, "Using a machine learning approach for analysis of polling systems with correlated arrivals," in *DCCN*, 2021.
- [35] Z. Liu, P. Nain, and D. Towsley, "On optimal polling policies," *Queueing Syst*, vol. 11, pp. 59–83, 1992.
- [36] H. Sato, Y. Matsumoto, and N. Okino, "The effect of recurrent networks on policy improvement in polling systems," in *ICANNGA*, 1997.
- [37] A. S. Matveev and R. Ishchenko, "Near-optimality of special periodic protocols for fluid models of single server switched networks with switchover times," *International Journal of Control*, vol. 90, pp. 2415 – 2432, 2017.
- [38] S. C. Borst and O. J. Boxma, "Polling: past, present, and perspective," *TOP*, vol. 26, pp. 335–369, 2018.
- [39] M. Malmirchegini and Y. Mostofi, "On the spatial predictability of communication channels," *IEEE Trans. on Wireless Commun.*, 2012.
- [40] Y. Mei, Y. Lu, Y. Hu, and C. Lee, "Deployment of mobile robots with energy and timing constraints," *IEEE Trans. on Robot.*, 2006.

- [41] H. Takagi, *Analysis of polling systems*. MIT Press, 1986.
- [42] B. Avi-Itzhak, H. Levy, and D. Raz, “Quantifying fairness in queuing systems: Principles, approaches, and applicability,” *Probability in the Engineering and Informational Sciences*, vol. 22, no. 4, p. 495–517, 2008.
- [43] G. Shapira and H. Levy, “On fairness in polling systems,” *Annals of Operations Research*, pp. 1–33, 2016.
- [44] D. Bertsimas and H. Xu, “Optimization of polling systems and dynamic vehicle routing problems on networks,” Sloan School of Management and Operations Research Center, MIT, Tech. Rep., 1993.
- [45] H. Edelsbrunner, D. Kirkpatrick, and R. Seidel, “On the shape of a set of points in the plane,” in *IEEE Trans. Inf. Theory*, 1983.
- [46] U. Ramer, “An iterative procedure for the polygonal approximation of plane curves,” *Comput. Graph. Image Process.*, vol. 1, pp. 244–256, 1972.
- [47] D. H. Douglas and T. Peucker, “Algorithms for the reduction of the number of points required to represent a digitized line or its caricature,” *Cartographica: The Inter. J. for Geographic Inf. and Geovisualization*, vol. 10, pp. 112–122, 1973.
- [48] S. Hertel and K. Mehlhorn, “Fast triangulation of simple polygons,” in *Found. of Computation Theory*, 1983.
- [49] A. Itai and Z. Rosberg, “A golden ratio control policy for a multiple-access channel,” *IEEE Trans. on Autom. Control*, vol. 29, pp. 712–718, 1984.
- [50] W. M. Smith, “Urban propagation modeling for wireless systems,” Ph.D. dissertation, Stanford University, 2004.
- [51] A. Gonzalez-Ruiz, A. Ghaffarkhah, and Y. Mostofi, “A Comprehensive Overview and Characterization of Wireless Channels for Networked Robotic and Control Systems,” *Journal of Robotics*, vol. 5, p. 19, 2011.
- [52] S. K. K. Hari, S. Rathinam, S. Darbha, K. Kalyanam, S. G. Manyam, and D. W. Casbeer, “The generalized persistent monitoring problem,” *2019 American Control Conference (ACC)*, pp. 2783–2788, 2019.
- [53] —, “Optimal uav route planning for persistent monitoring missions,” *IEEE Transactions on Robotics*, vol. 37, pp. 550–566, 2021.
- [54] J. Huang and R. Sengupta, “System time distribution of dynamic traveling repairman problem under the part-n-tsp policy,” *2015 European Control Conference (ECC)*, pp. 2762–2767, 2015.
- [55] L. Kleinrock and H. Levy, “The analysis of random polling systems,” *Oper. Res.*, vol. 36, pp. 716–732, 1988.